

Synthesis, Structure, and Catalytic Activity of Mononuclear Iron and (μ -Oxo)diiron Complexes with the Ligand 2,6-Bis(*N*-methylbenzimidazol-2-yl)pyridine

Ximeng Wang,^{*,†} Shuangxi Wang,[‡] Lijuan Li,^{*,†} Eric B. Sundberg,[†] and Gian Paola Gacho[†]

Department of Chemistry and Biochemistry, California State University, Long Beach, California 90840, and School of Medicine, University of California, Los Angeles, California 90095

Received August 9, 2002

Iron complexes including polyimidazole and exchangeable ligands are studied with the aim of modeling the structural and functional features of the non-heme iron centers of dinuclear proteins, such as methane monooxygenase. In $[\text{Fe}_2\text{OL}_2(\text{MeOH})_2(\text{NO}_3)_2](\text{NO}_3)_2$ (**1**) (L = 2,6-bis(*N*-methylbenzimidazol-2-yl)pyridine), each Fe(III) is in a distorted octahedral environment and has a donor set of N_3O_3 which includes three N atoms from L and three O atoms from a nitrate, μ -oxo, and methanol. In complex $[\text{Fe}(\text{LCl}_3)]$ (**2**) (L = 2,6-bis(*N*-methylbenzimidazol-2-yl)pyridine), Fe(III) is coordinated to three nitrogen atoms from L and three chloride ions. Complex **1** efficiently catalyzed the oxidation of cyclohexane with 51% conversion to cyclohexanol. It also catalyzed the epoxidation of styrene, cyclohexane, 2-methyl-2-butene, and *cis*- and *trans*-2-heptene with 51–84% conversions and high selectivity (71–99%) for epoxide products. Complex **2**, however, has no specific reactivity toward these substrates. From the alcohol/ketone (A/K) ratio close to 1 in the oxidation of cyclohexane, the low KIE (kinetic isotope effect K_H/K_D ratio = 1.8) for cyclohexanol formation, and the nonstereospecificity of the oxidation of *cis*-dimethylcyclohexane, it can be concluded that long-lived alkyl radicals are involved in the oxidation catalyzed by complex **1**. On the other hand, the stereospecific epoxidation of alkenes, the stereoselective oxidation of cumene, and the high degree of retention of configuration in the oxidation of *cis*- and *trans*-2-heptene suggest that a nonradical species, probably a metal-based intermediate, is involved in the oxidation of alkenes and cumene.

Introduction

Oxo- and hydroxo-bridged diiron sites occur in several proteins involved in reversible dioxygen binding or activation.¹ Significant examples of this class include the following: hemerythrin (Hr), which binds dioxygen reversibly; the R2 subunit of ribonucleotide reductase (RNR) from *Escherichia coli*; the soluble form of methane monooxygenase (MMO+), which consumes dioxygen to generate a tyrosyl radical and convert methane to methanol. Over the past few years a large number of μ -oxo-bridged diiron complexes have been prepared as structural models of the active sites in these proteins.^{2–7} Recently, much focus has been directed toward

the synthesis of models that are capable of mimicking the alkane functionalization chemistry of methane monooxygenase.⁸ These studies include the following systems: $[\text{Fe}_2\text{O}(\text{TPA})_2(\text{H}_2\text{O})_2]^{4+}/t\text{-BuOOH}(\text{H}_2\text{O}_2)$;⁹ $[\text{Fe}_2\text{O}(\text{L})_4\text{X}_n]^{m+}/t\text{-BuOOH}$

* To whom correspondence should be addressed. E-mail: xwang@csulb.edu (X.W.); lli@csulb.edu (L.L.).

[†] California State University at Long Beach.

[‡] University of California at Los Angeles.

- (1) (a) Nordlund, P.; Eklund, H. *Curr. Opin. Struct. Biol.* **1995**, *5*, 758. (b) Wallar, B. J.; Lipscomb, J. D. *Chem. Rev.* **1996**, *96*, 2625. (c) Feig, A. L.; Lippard, S. J. *Chem. Rev.* **1994**, *94*, 759.

- (2) Lippard, S. J. *Angew. Chem., Int. Ed. Engl.* **1988**, *27*, 344.
 (3) Sanders-Loehr, J. In *Iron Carriers and Iron Proteins*; Loehr, T. M., Ed.; VCH Press: New York, 1989; pp 373–466.
 (4) Vincent, J. B.; Olivier-Lilley, G. L.; Averill, B. A. *Chem. Rev.* **1990**, *90*, 1447.
 (5) Kurtz, D. M., Jr. *Chem. Rev.* **1990**, *90*, 585.
 (6) Que, L., Jr.; True, A. E. *Prog. Inorg. Chem.: Bioinorg. Chem.* **1990**, *38*, 97.
 (7) Que, L., Jr. In *Bioinorganic Catalysis*; Reedijk, J., Ed.; Dekker: New York, 1993; pp 347–393.
 (8) (a) Fontecave, M.; Menage, S.; Duboc-Toia, C. *Coord. Chem. Rev.* **1998**, *178–180*, 1555. (b) Costas, M.; Chen, K.; Que, L., Jr. *Coord. Chem. Rev.* **2000**, *200–202*, 517.
 (9) (a) Kim, J.; Harrison, R. G.; Kim, C.; Que, L., Jr. *J. Am. Chem. Soc.* **1996**, *118*, 4373. (b) Kim, J.; Larka, E.; Wilkinson, E. C.; Que, L., Jr. *Angew. Chem., Int. Ed. Engl.* **1995**, *34*, 2048. (c) Kojima, T.; Leising, R. A.; Yan, S.; Que, L., Jr. *J. Am. Chem. Soc.* **1993**, *115*, 11328. (d) Leising, R. A.; Kim, J.; Perez, M. A.; Que, L., Jr. *J. Am. Chem. Soc.* **1993**, *115*, 9524.

(where L = bipy, 4,4'-(Me)₂-bipy, phen; X = H₂O, Cl, OAc, CF₃CO₂);¹⁰ [Fe₂O(OAc)₂(bipy)₂Cl₂]/*t*-BuOOH (or H₂O₂);¹¹ [Fe₂O(OAc)(tmima)₂]³⁺/H₂O₂;^{11a} [Fe₂O(H₂O)₂(tmima)₂]⁴⁺/H₂O₂;¹² [Fe₂O(HB(pz)₃)₂(X)₂]/Zn/O₂ (X=OAc, Hfacac);¹³ [Fe₂O(salen)₂]/2-mercaptoethanol/O₂;¹⁴ [Fe₂OL₄(H₂O)₂](ClO₄)₄ (L = L(-)-4,5-pinenebipyridine);¹⁵ [Fe^{II}(TPA)(MeCN)₂]²⁺/*t*-BuOOH (H₂O₂).¹⁶

Fontecave and co-workers^{11b} studied the correlation between non-heme dinuclear iron functional models for MMO and their catalytic activity during the activation of C–H bonds by hydroperoxides. It was found that this activity requires the presence of an exchangeable coordination site that allows the oxidant to bind to the metal center and that it can be finely tuned by small modifications of the iron environment. Bearing these results in mind, we have synthesized the μ -oxo-bridged diiron(III) complex [Fe₂O-(L)₂(MeOH)₂(NO₃)₂](NO₃)₂ (**1**) (L = 2,6-bis(*N*-methylbenzimidazol-2-yl)pyridine), which includes two exchangeable ligands, MeOH and NO₃⁻, per iron center, in the hope that it can serve as an efficient catalyst for the functionalization of hydrocarbons. In this paper we describe the syntheses and structures of the singly μ -oxo-bridged [Fe₂O(L)₂(MeOH)₂(NO₃)₂](NO₃)₂ (**1**) and the mononuclear [Fe(L)(Cl)₃] (**2**) complexes and discuss their catalytic activity during the oxidation of alkanes and alkenes in the presence of *t*-BuOOH or H₂O₂.

Experimental Section

Reagents. All chemicals were of reagents grade unless otherwise noted. The solvents were purified by standard procedures. The ligands 2,6-bis(*N*-methylbenzimidazol-2-yl)pyridine (L),¹⁷ (Et₄N)₂(Fe₂-

OCl₆),¹⁸ and [Fe₃O(OAc)₆(H₂O)₃](NO₃)₃¹⁹ were synthesized according to published procedures.

Preparation of [Fe₂O(L)₂(NO₃)₂(CH₃OH)₂](NO₃)₂ (1**). Method A.** A mixture of L (165 mg, 0.5 mmol) and Fe(NO₃)₃·9H₂O (202 mg, 0.5 mmol) in methanol (40 mL) was refluxed for 3 h. The resulting orange-red solution was filtered to remove insoluble solids. The filtrate was allowed to stand at room temperature for several hours, after which time it yielded orange-red crystals (yield: 81%). Anal. Calcd for C₄₄H₄₂Fe₂N₁₄O₁₅: C, 47.23; H, 3.76; N, 17.53. Found: C, 47.38; H, 3.55; N, 17.08. FT-IR (KBr pellet), selected peaks: 1481 (s), 1385 (s), 1315 (s), 842 (s) and 820 (s) cm⁻¹. UV/vis (in CH₃OH, nm), λ_{\max} : 293 (ϵ_{\max} 5700 M_{Fe}⁻¹ cm⁻¹), 355 (ϵ_{\max} 1200 M_{Fe}⁻¹ cm⁻¹), 542 (ϵ_{\max} 280 M_{Fe}⁻¹ cm⁻¹), 705 (ϵ_{\max} 80 M_{Fe}⁻¹ cm⁻¹) nm. Raman (in MeOH): $\nu_{\text{asym}}(\text{Fe}-\text{O}-\text{Fe}) = 352$ cm⁻¹. Mössbauer (solid state): $\delta = 0.46$ mm s⁻¹, $\Delta E_Q = 1.27$ mm s⁻¹.

Method B. A mixture of L (509 mg, 1.5 mmol) and [Fe₃O(OAc)₆(H₂O)₃](NO₃)₃ (327 mg, 0.5 mmol) in 50 mL of methanol/water (1:1 v/v) was refluxed for 1 h. **1** was obtained as orange-red crystals (yield: 61% based on the ligand used) upon cooling at room temperature.

Preparation of Fe(L)Cl₃ (2**).** (Et₄N)₂(Fe₂OCl₆) (115 mg, 0.19 mmol) was added to a solution of L (130 mg, 0.38 mmol) in methanol (25 mL) while stirring at room temperature. An orange-red precipitate immediately formed. After the mixture was stirred for 2 h, the precipitate was collected by filtration, washed with ethanol and diethyl ether, and dried in a vacuum over P₄O₁₀. Anal. Calcd for C₂₁H₁₇Cl₃FeN₅: C, 50.25; H, 3.39; N, 13.96. Found: C, 49.81; H, 3.41; N, 13.82. UV/vis (in CH₃OH, nm), λ_{\max} : 294 (ϵ_{\max} 5800 M_{Fe}⁻¹ cm⁻¹), 358 (ϵ_{\max} 1300 M_{Fe}⁻¹ cm⁻¹).

Oxidation of Hydrocarbon Substrates. All manipulations were performed under a dioxygen-free N₂ atmosphere. In a typical reaction, complex **1** or **2** (0.02 mmol) in 10 mL of CH₃CN and 45 mmol of substrate were mixed. After the mixture was stirred for 10 min, the reaction was started by the addition of 50 mmol of *t*-BuOOH (5–6 M in nonane) or H₂O₂ (30% in water) and stirred under N₂ atmosphere at 35 °C for 2–3 h. The organic products were identified by GC, using authentic compounds as internal standards, and further verified by GC/MS and ¹H NMR spectra.

Kinetic Isotope Effect Determination. In the same procedure described above, a cyclohexane/(D₁₂)cyclohexane (ratio 1:1) mixture was used. We quantitated the products by GC (acetophenone as standard). The KIE was determined by comparing the yields for cyclohexanol and (D₁₁)cyclohexanol and corrected for the relative concentrations of cyclohexane and (D₁₂)cyclohexane.

Collection and Reduction of X-ray Data. Single crystals of **1** were obtained directly from the reaction medium, while single crystals of **2**·CH₃OH were obtained by slow vapor diffusion of diethyl ether into the methanol solution. The crystals of **1** and **2**·CH₃OH are both air stable. All crystal data for complexes **1** and **2**·CH₃OH were collected at 298 K on an Enraf-Nonius CAD 4 diffractometer using graphite-monochromated Mo K α ($\lambda = 0.71073$ Å) radiation. The unit cell dimensions were obtained from a least-squares fit of 25 reflections with 5° < 2 θ < 24° for **1** and 8° < 2 θ < 25° for **2**·CH₃OH. A summary of the crystal data, intensity measurement, and solution refinements is given in Table 1. Five standard reflections monitored periodically during data collection showed that the variations for **1** and **2**·CH₃OH are less than 2.2% and 1.2%, respectively. All data were corrected for Lorentz and

- (10) Abbreviations used: TPA, tris(2-pyridylmethyl)amine; tmima, tris((1-methylimidazol-2-yl)methyl)amine; HB(pz)₃, hydrotris(pyrazolyl)borate; hfacac, hexafluoroacetylacetonate; salen, *N,N'*-bis(salicylidene)ethylenediamine; N₅, *N,N,N',N',N'*-tris(benzimidazol-2-ylmethyl)-*N'*-(2-hydroxyethyl)ethane-1,2-diamine; BBA, bis(benzimidazol-2-ylmethyl)amine; TBHP, *N,N,N',N'*-tetrakis(benzimidazol-2-ylmethyl)-2-hydroxy-1,3-diaminopropane; phen, 1,10-phenanthroline; IIIa, 2-(5-phenylpyrazol-3-yl)phenol.
- (11) (a) Menage, S.; Wilkinson, E. C.; Que, L., Jr. Fontecave, M. *Angew. Chem., Int. Ed. Engl.* **1995**, *34*, 203. (b) Menage, S.; Vincent, J. M.; Lambeaux, C.; Chottard, G.; Grand, A.; Fontecave, M. *Inorg. Chem.* **1993**, *32*, 4766. (c) Meckmouche, Y.; Ménage, S.; Toia-Duboc, C.; Fontecave, M.; Galey, J.-B.; Lebrun, C.; Pécaut, J. *Angew. Chem., Int. Ed.* **2001**, *40*, 949.
- (12) (a) Fish, R. H.; Konings, M. S.; Oberhausen, K. J.; Fong, R. H.; Yu, W. M.; Christou, G.; Vincent, J. B.; Coggin, D. K.; Buchanan, R. M. *Inorg. Chem.* **1991**, *30*, 3002. (b) Vincent J. B.; Huffman, J. C.; Christou, G.; Li, Q.; Nanny, M. A.; Hendrickson, D. N.; Fong, R. H.; Fish, R. H. *J. Am. Chem. Soc.* **1988**, *110*, 6898. (c) Buchanan, R. M.; Chen, S.; Richardson, J. F.; Bressan, M.; Forti, L.; Morvillo, A.; Fish, R. H. *Inorg. Chem.* **1994**, *33*, 3208.
- (13) (a) Kitajima, N.; Ito, M.; Fukui, H.; Moro-oka, Y. *J. Chem. Soc., Chem. Commun.* **1991**, 102. (b) Kitajima, N.; Fukui, H.; Moro-oka, Y. *J. Chem. Soc., Chem. Commun.* **1988**, 485.
- (14) Tabushi, I.; Nakajima, T.; Seto, K. *Tetrahedron Lett.* **1980**, *21*, 2565.
- (15) (a) Mekmonche, M.; Hummel, H.; Ho, R. Y. N.; Que, L., Jr.; Schunemann V.; Thomas, F.; Trautwein, A. X.; Lebrun, C.; Gorgy, K.; Lepretre, J.-C.; Collomb, M.-N.; Deronzier, A.; Fontecave, M.; Menage S. *Chem.—Eur. J.* **2002**, *8*, 1196. (b) Duboc-Toia, C.; Menge, S.; Ho, R. Y. N.; Que, L., Jr.; Lambeaux, C.; Fontecave, M. *Inorg. Chem.* **1999**, *38*, 1261.
- (16) (a) Chen, K.; Que, L., Jr. *J. Am. Chem. Soc.* **2001**, *123*, 6327. (b) Chen, K.; Que, L. Jr. *Angew. Chem., Int. Ed.* **1999**, *38*, 2227. (c) Kim, C.; Chen, K.; Kim, J.; Que, L., Jr. *J. Am. Chem. Soc.* **1997**, *119*, 5964. (d) Roelfes, G.; Lubben, M.; Hage, R.; Que, L., Jr.; Feringa, B. L. *Chem.—Eur. J.* **2000**, *6*, 2152.

- (17) Piguet, C.; Bocquet, B.; Muler, E.; Williams, A. F. *Helv. Chim. Acta* **1989**, *72*, 323.
- (18) Armstrong, W. H.; Lippard, S. J. *Inorg. Chem.* **1985**, *24*, 981.
- (19) Taft, K. L.; Masschelein, A.; Liu, S.; Lippard, S. J.; Garfinkel-Shweky, D.; Bino, A. *Inorg. Chim. Acta* **1992**, *198–200*, 673.

Table 1. Data Collection and Parameters for Complexes **1** and **2**·CH₃OH

	1	2 ·CH ₃ OH
formula	C ₄₄ H ₄₂ Fe ₂ N ₁₄ O ₁₅	C ₂₂ H ₂₁ FeN ₅ O
fw	1118	534
cryst system	monoclinic	monoclinic
space group	<i>P</i> 2 ₁ / <i>n</i>	<i>P</i> 2 ₁ / <i>n</i>
<i>a</i> , Å	10.990 (2)	11.817 (6)
<i>b</i> , Å	14.024 (3)	13.922 (2)
<i>c</i> , Å	15.859 (3)	14.034 (6)
β , deg	105.78 (1)	103.84 (3)
<i>V</i> , Å ³	2352 (1)	2242 (2)
<i>Z</i>	2	4
<i>T</i> , °C	23	23
cryst color	red	red
<i>d</i> (calcd), g cm ⁻³	1.60	1.58
μ (Mo K α), cm ⁻¹	7.0	10.57
2 θ max, deg	50	50
unique reflns	3691	4155
reflncs with <i>I</i> > 3 σ (<i>I</i>)	2484	3111
no. of variables	337	289
<i>R</i> ^a	0.064	0.039
<i>R</i> _w ^a	0.074	0.051

$$^a R = \sum ||F_o| - |F_c|| / \sum |F_o|. R_w = [\sum w(|F_o| - |F_c|)^2 / \sum w F_o^2]^{1/2}, w = 1/\sigma^2(F_o) = 4F_o^2/\sigma^2(F_o^2).$$

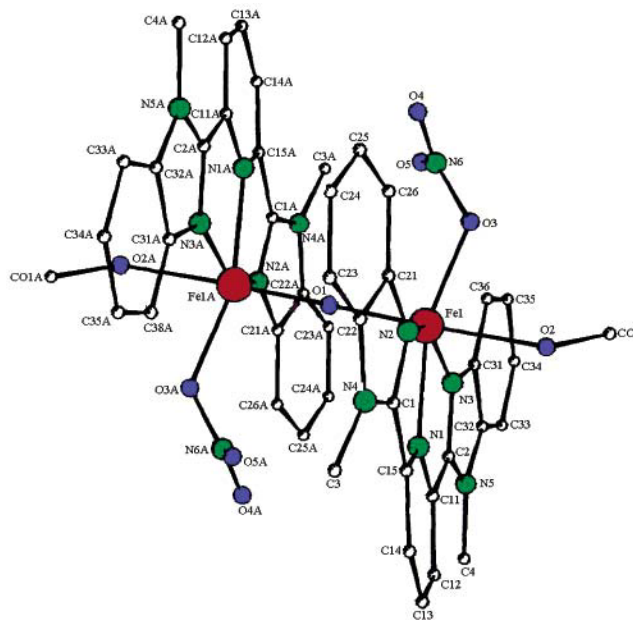
polarization effects. An empirical absorption correction based on the φ plot was applied.²⁰

Structure Solution and Refinement. The structures for **1** and **2**·CH₃OH were solved by direct methods and successive Fourier-difference syntheses and refined by full-matrix least-squares methods. All the hydrogen atoms were generated geometrically and included isotropically in the structure factor calculations, but they were not refined. Atomic scattering factors were taken from The International Tables for X-ray Crystallography.²¹ All calculations were performed with the SHELXTL program.²²

Physical Measurements. Microanalyses (C, H, N) were performed with a Carlo-Eiba 1106 elemental analyzer. The IR spectra of samples in KBr disks were recorded on a Nicolet-170 SX FT-IR spectrometer in the 4000–400 cm⁻¹ range. The ¹H NMR spectra were recorded with a Bruker AM-80 spectrometer. The Raman spectra were recorded on a 14031 laser spectrometer with 457.9 nm excitation. Mass spectra were obtained on an AEI-MS-902 mass spectrophotometer. All UV/vis spectra of samples in CH₃CN were recorded on a Shimadzu model UV-240 spectrophotometer in the 190–900 nm region.

Mössbauer Spectroscopy. The Mössbauer spectrum was obtained at room temperature using a Hadler MR-351 type spectrometer. A 10 mCi (3.7 × 10⁸ Bq) ⁵⁷Co (Rh) source was used. Each spectrometer was calibrated with respect to standard stainless steel at room temperature. The spectrum was fitted by Lorentzian line shapes using least-squares methods.

Magnetic Studies. Magnetic susceptibility measurements were carried out using a CAHN-200 Faraday-type magnetometer operating at 50 KG (5T) in the 3–300 K range. A powder sample of complex **1** was placed in a Kelf bucket, which had been calibrated independently. Diamagnetic contributions were evaluated using Pascal's constants.²³ The data were fitted to the equation for isotropic exchange ($-2J_1S_1S_2$) in a *S*₁ = *S*₂ = 5/2 spin system²⁴


Figure 1. ORTEP drawing for [Fe₂OL₂(MeOH)₂(NO₃)₂](NO₃)₂ (**1**) with thermal ellipsoids drawn at the 50% probability level.

modified to allow for a mixture of paramagnetic impurities (*P*%). The temperature-independent paramagnetic (TIP) susceptibility term results from the mixing of nonthermally populated wave functions of low-lying excited states into the ground-state wave functions. The value minimized was $R = \sum (\chi_{\text{exptl}} - \chi_{\text{calc}})^2 / n \sum \chi_{\text{exptl}}^2$, where *n* is the number of data used.

Results and Discussion

Synthesis. The μ -oxo-bridged diiron complex **1** with methanol and nitrate as monodentate terminal ligands was obtained readily by refluxing a reaction mixture of L with Fe(NO₃)₃·9H₂O, or with [(Fe₃O)(OAc)₆(H₂O)₃](NO₃) in methanol or a methanol–water solution. The yields were 81% and 61% (based on the ligand used), respectively. Attempts to synthesize the μ -oxo-bridged diiron complex [Fe₂O(L)₂Cl₄] with Cl⁻ as a terminal ligand were unsuccessful, even when the μ -oxo-bridged diiron [Fe₂OCl₆]²⁻ complex was used as starting material. The mononuclear complex **2** was the only product obtained. Complexes **1** and **2** are stable in air and over a large temperature range, and they are soluble in methanol and acetonitrile.

Description of the Structures. [Fe₂O(L)₂(NO₃)₂(CH₃OH)₂](NO₃)₂ (**1**). The structure of complex **1** consists of the [Fe₂O(L)₂(NO₃)₂(CH₃OH)₂]²⁺ cation and NO₃⁻ counteranions. A view of the centrosymmetric cation is shown in Figure 1. Selected bond lengths and angles are summarized in Table 2. The bridging oxo group (O(1)) lies on the crystallographic center of symmetry that relates both halves of the molecule. Each iron atom sits in a N₃O₃ donor set and has a distorted octahedral geometry. Three N atoms come from the tridentate planar ligand L and three O atoms come from the bridging oxo group, the nitrate, and the methanol. The Fe–N(benzimidazole) bond lengths (2.113(5) and 2.118(5) Å) are longer than those found in [N₅FeOFeCl₃]⁺ (where N₅ = N, N', N'')

(24) O'Connor, C. J. *Prog. Inorg. Chem.* **1982**, 29, 203.

(20) North, A. C. T.; Phillips, D. C.; Mathews, F. S. *Acta Crystallogr.* **1968**, A24, 351.

(21) *International Tables for X-ray Crystallography*; Kynoch Press: Birmingham, U.K., 1974; Vol. 4.

(22) Sheldrick, G. M. *SHELXTL, System for Crystal Structure Solution, Revision 5.1*; University of Göttingen: Göttingen, Germany, 1986.

(23) Carlin, R. L. *Magnetochemistry*; Springer-Verlag: Berlin, 1986; pp 33 and 64.

Table 2. Selected Bond Lengths (Å) and Bond Angles (deg) for Complex **1**

Fe(1)–N(1)	2.164(5)	Fe(1)–O(1)	1.773(1)
Fe(1)–N(2)	2.113(5)	Fe(1)–O(2)	2.157(5)
Fe(1)–N(3)	2.118(5)	Fe(1)–O(3)	2.000(5)
Fe(1)–O(1)–Fe(1*)	180.0	O(1)–Fe(1)–O(2)	176.9(1)
O(1)–Fe(1)–O(3)	98.9(2)	O(1)–Fe(1)–N(2)	93.6(1)
O(1)–Fe(1)–N(1)	100.6(1)	O(1)–Fe(1)–N(3)	98.7(2)
O(2)–Fe(1)–N(1)	81.0(2)	O(3)–Fe(1)–N(1)	160.4(2)
O(3)–Fe(1)–N(2)	101.9(2)	O(3)–Fe(1)–N(3)	105.4(2)
O(3)–Fe(1)–O(2)	79.5(2)	N(2)–Fe(1)–N(3)	147.8(2)
N(2)–Fe(1)–O(2)	84.3(2)	N(2)–Fe(1)–N(1)	74.3(2)
N(3)–Fe(1)–O(2)	84.2(2)	N(3)–Fe(1)–N(1)	74.2(2)

Table 3. Selected Bond Lengths (Å) and Bond Angles (deg) for Complex **2**·CH₃OH

Fe–N(1)	2.111(3)	Fe–Cl(3)	2.234(1)
Fe–N(5)	2.124(3)	Fe–Cl(2)	2.326(1)
Fe–N(3)	2.168(3)	Fe–Cl(1)	2.427(1)
N(1)–Fe–N(5)	147.4(1)	N(1)–Fe–N(3)	73.6(1)
N(1)–Fe–Cl(3)	106.39(8)	N(1)–Fe–Cl(2)	91.49(8)
N(1)–Fe–Cl(1)	88.14(8)	N(5)–Fe–N(3)	73.9(1)
N(5)–Fe–Cl(3)	106.13(8)	N(5)–Fe–Cl(2)	86.23(8)
N(5)–Fe–Cl(1)	90.63(8)	N(3)–Fe–Cl(3)	173.89(8)
N(3)–Fe–Cl(2)	89.77(8)	N(3)–Fe–Cl(1)	83.98(8)

tris[(benzimidazol-2-yl)methyl]-*N'*-(2-hydroxyethyl)ethane-1,2-diamine (average 2.094 Å)²⁵ and comparable to [Fe₂O(O₂CPh)₂(BBA)₂]²⁺ (BBA = bis[(benzimidazol-2-yl)methyl]amine) (2.112 Å)²⁶ but shorter than those found in [Fe₄O₂(O₂CPh)(TBHP)₂]⁴⁺ (TBHP = *N,N,N',N'*-tetrakis[(benzimidazol-2-yl)methyl]-2-hydroxy-1,3-diaminopropane) (2.185 Å).²⁷ The Fe–N(pyridine) bond length (2.164(5) Å) is significantly longer than the Fe–N(benzimidazole) bond lengths observed in complex **2**·CH₃OH (Table 3). In general, *N*-imidazole is a good π donor ligand compared to *N*-amine and *N*-pyridine and, therefore, has shorter metal–ligand bond lengths.²⁸ The Fe–O(nitrate) bond (2.005(5) Å) is shorter than those found in other Fe complexes (2.103(5)–2.262(2) Å).²⁹ The methanol ligand is coordinated to the Fe center with an Fe–O bond distance of 2.157 Å, which is significantly longer than the other Fe–O or Fe–N bond distances in **1**. It is also longer than the 2.136(5) and 2.094(3) Å values found in the mononuclear complexes [FeCl₃(phen)(MeOH)]³⁰ and (Fe(IIIa)₂(MeOH)₂NO₃·MeOH (IIIa = 2-(5-phenyl)pyrazol-3-yl)phenol),³¹ respectively, because of the trans influence of the short Fe–O_{oxo} bond. The oxo Fe–O bond length (1.773(1) Å) is in the range found for other μ -oxo diiron complexes (1.75–1.80 Å) and is very close to the oxo Fe–O values observed in methemerythrin and methmyohemerythrin azide, which average 1.78 Å.⁶

The Fe–O–Fe bond angle is 180°, and the Fe···Fe separation is 3.546 Å. The two planar ligands, with maximum deviation of 0.2 Å from the least-squares planes in **1**, are transoid to the oxo bridge and parallel to each other. This causes significant π – π stacking interaction between the two parallel planar rings of the ligands (Figure 2). The π – π stacking distance between the two planes is 3.546 Å, which is close to the 3.35 Å known for graphite sheets³² and the 3.4 Å for stacked nucleotide residues in DNA.³³ Interligand π – π stacking interactions are becoming increasingly common in coordination complexes involving aromatic ligands³⁴ and have been used to control binding of aromatic substrates in host–guest systems.³⁵ The theoretical estimation of the magnitude of these interactions is still sparse, but recently it has been shown that face-to-face (rather than edge-to-edge) stacking is favored when the size of the aromatic system is increased.³⁶ This interligand π -stacking interaction participates in the stability of singly oxo-bridged diiron complexes^{37–39} and may explain the short Fe–O_{oxo} value in **1**. To the best of our knowledge, this is the first structurally characterized (μ -oxo)diiron complex with a tridentate planar ligand and methanol coordination. Reiff and co-workers⁴⁰ have reported a (μ -oxo)diiron complex with a planar terpy ligand, formulated as [Fe₂O(terpy)₂](NO₃)₄·4H₂O, which was only characterized by spectroscopic methods. It is reasonable to assume that this complex has a structure similar to that of **1**.

Fe(L)Cl₃·CH₃OH (2·CH₃OH). A perspective view of the molecule with the atomic numbering scheme is shown in Figure 3. Selected bond lengths and angles are summarized in Table 3. The molecule is a neutral Fe(III) complex in which Fe is hexacoordinated with a distorted octahedral geometry. The tridentate N₃ planar ligand (L) coordinates the iron(III) center in a meridional fashion. The three monodentate chloride ligands occupy the remaining meridional sites. The Fe–N(benzimidazole) distances (2.111(3), 2.124(3) Å) are shorter than the Fe–N(pyridine) distance (2.168(3) Å) as observed in a related manganese complex.⁴¹ The Fe–Cl(equatorial) distance (2.234(1) Å) is, as expected,

- (25) Gómez-Romero, P.; Witten, E. H.; Reiff, W. M.; Backes, G.; Sanders-Loehr, J.; Jameson, G. B. *J. Am. Chem. Soc.* **1989**, *111*, 9039.
 (26) Gómez-Romero, P.; Casan-Pastor, N.; Ben-Hussein, A.; Jameson, G. B. *J. Am. Chem. Soc.* **1988**, *110*, 1988.
 (27) Chen, Q.; Lynch, J. B.; Gómez-Romero, P.; Ben-Hussein, A.; Jameson, G. B.; O'Connor, C. J.; Que, L., Jr. *Inorg. Chem.* **1988**, *27*, 2673.
 (28) Jones, C. M.; Johnson, C. R.; Asher, S. A.; Shepherd, R. E. *J. Am. Chem. Soc.* **1985**, *107*, 3772.
 (29) Plakatouras, J. C.; Bakas, T.; Huffman, C. J.; Huffman, J. C.; Papaefthymiou, V.; Perlepes, S. P. *J. Chem. Soc., Dalton Trans.* **1994**, 2737.
 (30) Healy, P. C.; Patrick, J. M.; Skelton, B. W.; White, A. H. *Aust. J. Chem.* **1983**, *36*, 2031.
 (31) Ainscough, E. W.; Brodie, A. M.; Plowman, J. E.; Brown, K. L.; Addison, A. W.; Gainsford, A. R. *Inorg. Chem.* **1980**, *19*, 3655.

- (32) Greenwood, N. N.; Earnshaw, A. *Chemistry of the Elements*; Pergamon Press: Oxford, U.K., 1984.
 (33) T'So, P. O. P., Ed. *Basic Principles in Nucleic Acid Chemistry*, 1st ed.; Academic Press: New York, 1974; Vol. 1.
 (34) (a) Constable, E. C.; Ward, M. D.; Tocher, D. A. *J. Chem. Soc., Dalton Trans.* **1991**, 1675. (b) Constable, E. C.; Elder, S. M.; Healy, J.; Ward, M. D. *J. Am. Chem. Soc.* **1990**, *112*, 4590. (c) Constable, E. C.; Elder, S. M.; Raithby, P. R.; Ward, M. D. *Polyhedron* **1991**, *10*, 1395. (d) Constable, E. C.; Holmes, J. M.; Raithby, P. R. *Polyhedron*, **1991**, *10*, 127. (e) Castonguay, L. A.; Rappe, A. K.; Casewit, C. J. *J. Am. Chem. Soc.* **1991**, *113*, 7177. (f) Schall, O. F.; Robinson, K.; Atwood, J. L.; Gokel, G. W. *J. Am. Chem. Soc.* **1991**, *113*, 7434.
 (35) (a) Zimmerman, S. C.; Wu, W. *J. Am. Chem. Soc.* **1989**, *111*, 8054. (b) Muehldorf, A. V.; Engen, D. V.; Warner, J. C.; Hamilton, A. D. *J. Am. Chem. Soc.* **1988**, *110*, 6561. (c) Diederich, F. *Angew. Chem., Int. Ed. Engl.* **1988**, *27*, 362.
 (36) Jorgensen, W. L.; Severance, D. L. *J. Am. Chem. Soc.* **1991**, *113*, 209.
 (37) Takahashi, K.; Nishida, Y.; Maeda, Y.; Kida, S. *J. Chem. Soc., Dalton Trans.* **1985**, 2375.
 (38) Plowman, J. E.; Loehr, T. M.; Schauer, C. K.; Anderson, O. P. *Inorg. Chem.* **1984**, *23*, 3553.
 (39) Buchanan, R. M.; O'Brien, R. J.; Richardson, J. F.; Latour, J. M. *Inorg. Chim. Acta* **1993**, *214*, 33.
 (40) Reiff, W. M.; Baker, W. A. Jr.; Erickson, N. E. *J. Am. Chem. Soc.* **1968**, *90*, 4794.

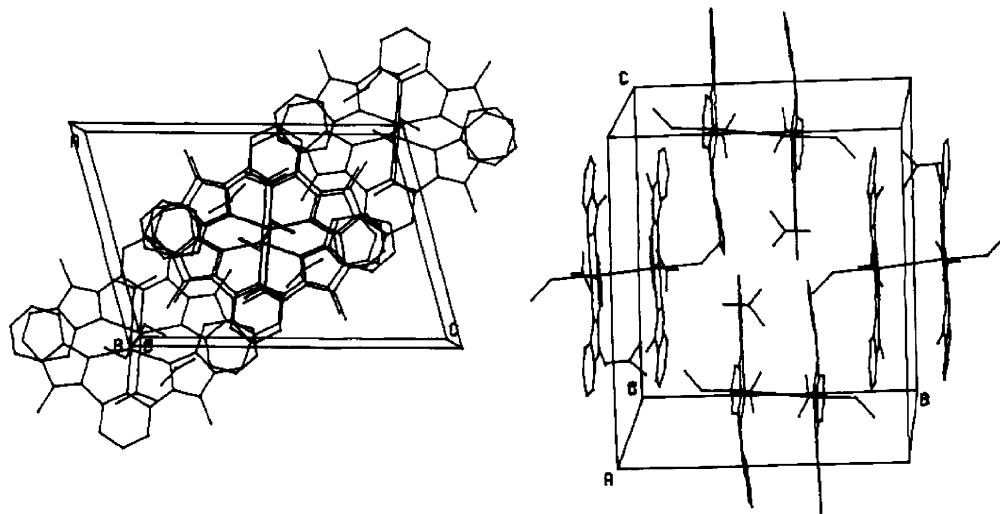


Figure 2. Perspective view of $[\text{Fe}_2\text{OL}_2(\text{MeOH})_2(\text{NO}_3)_2](\text{NO}_3)_2$ (**1**) showing the intermolecular π - π stacking.

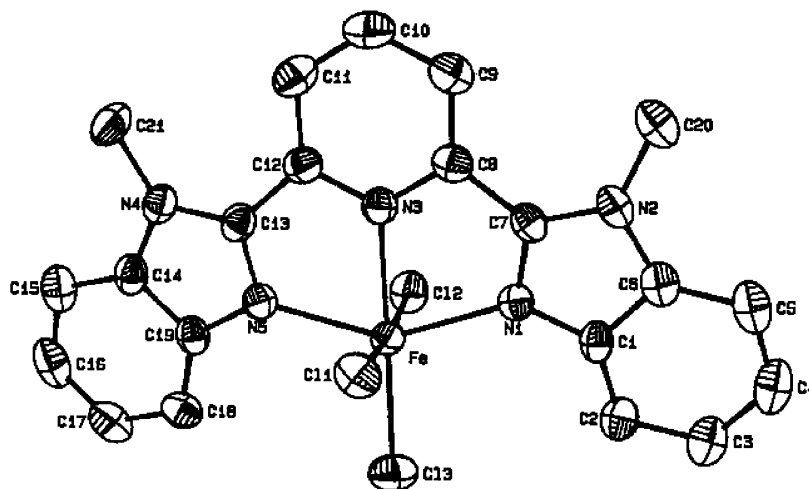


Figure 3. ORTEP drawing for (FeLCl_3) (**2**) with thermal ellipsoids drawn at the 50% probability level.

significantly shorter than the Fe-Cl(axial) distances (2.326(1), 2.427(1) Å). The angle Cl(2)-Fe-Cl(1) (173.58°) is close to the ideal value of 180° , while bond angles in the equatorial plane show large distortions from the ideal value of 90° (73.6 , 73.9 , 106.13 , and 88.14° for N(1)-Fe-N(3), N(3)-Fe-N(5), N(5)-Fe-Cl(3), and Cl(3)-Fe-N(1), respectively) due to the stereo requirement of L. The crystallographic study shows that the solvated molecule methanol in $\text{Fe}(\text{L})\text{Cl}_3 \cdot \text{CH}_3\text{OH}$ does not interact with any atom of $\text{Fe}(\text{L})\text{Cl}_3$. The molecular packing is mainly determined by van der Waals interactions.

Electronic Spectroscopy. The electronic spectra of **1** and **2** (10×10^{-4} M) recorded in methanol show the splitting of intraligand π - π^* transition at ~ 355 and ~ 293 nm, indicating that ligand L is coordinated to iron(III).¹⁵ Complex **1** also exhibits two bands at 542 and 705 nm, which are tentatively assigned to ${}^6\text{A}_1 \rightarrow ({}^4\text{A}_1, {}^4\text{E})$ and ${}^6\text{A}_1 \rightarrow {}^4\text{T}_2$, respectively.⁴²

Vibration Spectroscopy. In the IR spectrum of complex **1**, the Fe-O-Fe asymmetric stretching mode is assigned to the peak at 842 cm^{-1} on the basis of the literature reports.^{37,40} The nitrate groups in **1** yield three bands at 1482, 1351, and 820 cm^{-1} . The magnitude for the splitting of the two higher energy bands is 131 cm^{-1} , suggesting that nitrate groups are present as monodentate ligands.⁴³ Meanwhile, we observed the ionic nitrate band at 1385 cm^{-1} . These results show that complex **1** in methanol has both ionic and coordinated nitrate groups, which is consistent with the X-ray crystal structure. The resonance Raman spectrum of **1** was recorded with 457.9 nm excitation. The dominant feature at 352 cm^{-1} is the Fe-O-Fe symmetric stretching mode $\nu_{\text{sym}}(\text{Fe}-\text{O}-\text{Fe})$.⁴⁴ This result indicates that the (μ -oxo)diiron core of **1** is retained in methanol.

Mössbauer Spectroscopy. The Mössbauer spectrum of complex **1** was recorded at room temperature and shows an asymmetric quadruple doublet (Figure 4). The isomer shift

(41) Wang, S.; Zhu, Y.; Zhang, F.; Wang, Q.; Wang, L. *Polyhedron* **1992**, *11*, 1909.

(42) Norman, R. E.; Holz, R. C.; Menage, S.; Que, L., Jr.; Zhang, J. H.; O'Connor, C. J. *Inorg. Chem.* **1990**, *29*, 4629.

(43) Nakamoto, K. *Infrared and Raman Spectra of Inorganic and Coordination Compounds*, 4th ed.; Wiley: New York, 1986.

(44) Sanders-Loehr, J.; Wheeler, W. D.; Shiemke, A. K.; Averill, B. A.; Loehr, T. M. *J. Am. Chem. Soc.* **1989**, *111*, 8084.

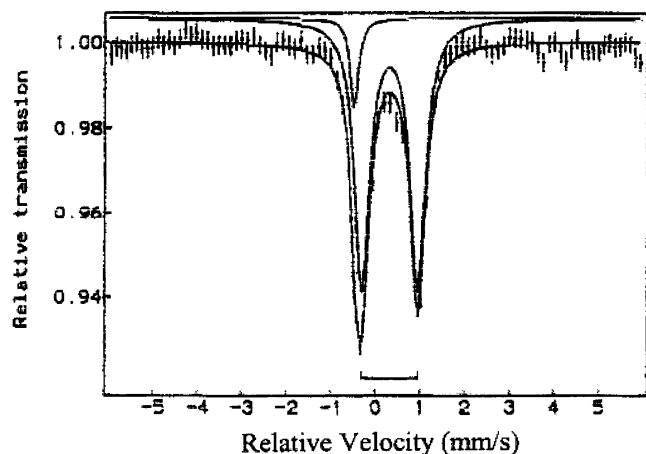


Figure 4. Mössbauer spectrum of complex **1** at room temperature.

and the quadruple splitting (ΔE_Q) for **1** are 0.46 and 1.27 mm s^{-1} , respectively. Since the isomer shifts for high-spin mononuclear and μ -oxo-bridged iron(III) complexes generally fall in the 0.3–0.6 mm s^{-1} range,⁴⁵ the 0.46 mm s^{-1} isomer shift obtained is consistent with the presence of high-spin iron(III) in **1**. The 1.27 mm s^{-1} quadruple splitting for **1** lies at the lower end of the 1.27–1.85 mm s^{-1} range found in other μ -oxo-bridged diiron(III) complexes, indicating a near symmetric charge distribution around the iron nucleus in **1**.⁴⁶

Magnetic Properties. The solution magnetic susceptibility measurement was carried out for **1** in acetonitrile solution using the Evans method.⁴⁷ An effective magnetic moment of 1.68 μ_B/Fe was obtained. This is much smaller than the 5.9 μ_B for high-spin mononuclear iron(III), indicating that the (μ -oxo)diiron(III) core of complex **1** is retained in solution. Solid-state variable-temperature magnetic susceptibility studies have been performed for **1**. A nonlinear least-squares fitting program⁴⁸ was used to fit the observed data. With g fixed at 2, optimization of the fit for **1** gave $J = -107.7 \text{ cm}^{-1}$, $P\% = 8.82 \times 10^{-2}$, $\text{tip} = 4.43 \times 10^{-5}$, and $R = 9.76 \times 10^{-3}$. A plot of molar magnetic susceptibility (χ_m) as a function of temperature is shown in Figure 5. The solid line represents the calculated data. The J value determined for **1** is in the -95 to -191 cm^{-1} range reported for singly oxo-bridged diiron complexes,⁵ but it is significantly smaller than the values (-187 , -191 cm^{-1}) reported for linear (μ -oxo)diiron porphyrin complexes.^{49a,b} In the latter case, the difference may be attributed to the slightly shorter Fe–O_{oxo} bond length in the linear (μ -oxo)diiron porphyrin complexes, because the J value for (μ -oxo)diiron complexes increases as the distance of the iron–oxo bond decreases.^{5,49c,d}

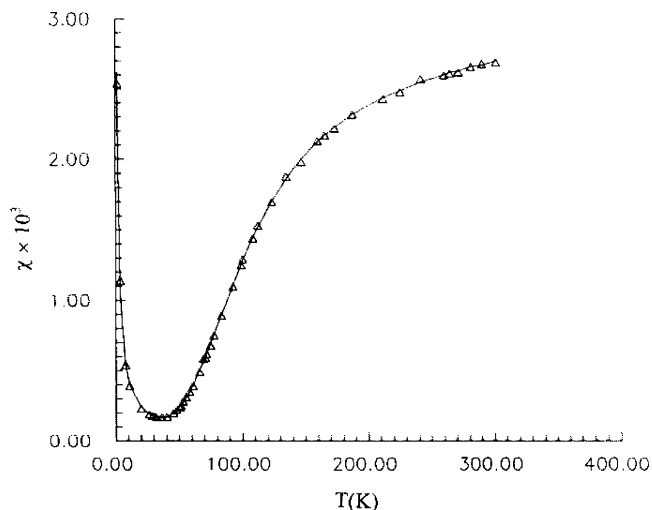


Figure 5. Molar susceptibility (Δ) for $[\text{Fe}_2\text{OL}_2(\text{MeOH})_2(\text{NO}_3)_2](\text{NO}_3)_2$ (**1**) as a function of temperature. The solid line is the theoretical fit.

Catalytic Activity of Complexes 1 and 2. The catalytic activity of complexes **1** and **2** was tested in the oxidation of cyclohexane, phenol, adamantane, and *cis*-1,2-dimethylcyclohexane by *tert*-butylhydroperoxide (*t*-BuOOH) and H_2O_2 in acetonitrile solutions at 35 °C under N_2 atmosphere. The product distributions are given in Table 4. Under our standard reaction conditions (complex **1** or **2**:substrate:oxidant ratio equal to 1:2250:2500), complex **1** catalyzes the oxidation of cyclohexane to cyclohexanol and cyclohexanone ($\sim 1:1$ ratio) with 51% conversion of the substrate. Under the same conditions, substrate (cyclohexane) conversion decreased to 37% when H_2O_2 was used. However, the ratio of cyclohexanol to cyclohexanone ($\sim 1:1$) was the same as with *t*-BuOOH. The addition of the tetrabutylammonium bromide (TBAB) phase-transfer catalyst to the H_2O_2 reaction mixture increased the conversion to 48%. Neither *t*-BuOOH nor H_2O_2 with complex **2** shows catalytic activity in the oxidation of cyclohexane. Both complexes **1** and **2**, under our reaction conditions, efficiently catalyze the oxidation of phenol to hydroquinone, with 61% and 23% conversions, respectively. Interestingly, a higher selectivity of the catalytic oxidizing system for the tertiary C–H bonds of adamantane with *t*-BuOOH by complex **1** has been observed. The C 3°/2° ratio is 15.4 (Table 4, entry 8). *cis*-1,2-Dimethylcyclohexane is converted into *cis*- and *trans*-1,2-dimethylcyclohexanol with a *cis/trans* ratio of 1.1 (Table 4, entry 9). The catalytic activities of complex **1** for the oxidation of several alkenes (styrene, 2-methyl-2-butene, cyclohexene, 1-methylcyclohexene, and *cis/trans*-2-heptenes) were determined. The product distributions are summarized in Table 5. Typical reactions with a ratio of catalyst **1**:substrate:*t*-BuOOH equal to 1:2250:2500 were run in acetonitrile solution for 2.5–3.0 h at 35 °C. Complex **1** catalyzes the oxidation of alkenes with 63–85% conversion to epoxides and ketones. However, the selectivity for epoxide formation is high. The product distributions (Table 5) for epoxides range from 77 to 99% and 0.3–7.9% for ketones or aldehydes. This high stereosepoxidation selectivity is in sharp contrast with the iron complex containing a tetradentate macrocyclic cyclam ligand

(45) Gibb, T. C.; Greenwood, N. N. In *Mössbauer Spectroscopy*; Chapman and Hall: London, 1971; pp 148–164.

(46) Adams, H.; Bailey, N. A.; Crane, J. D.; Fenton, D. E.; Latour, J.-M.; Williams, J. M. J. *Chem. Soc., Dalton Trans.* **1990**, 1727.

(47) Evans, D. F. *J. Chem. Soc.* **1959**, 2003.

(48) Wang, S.; Luo, Q.; Wang, X.; Wang, L.; Yu, K. *J. Chem. Soc., Dalton Trans.* **1995**, 2045.

(49) (a) Strauss, S. H.; Pawlik, M. J.; Skowyra, J.; Kennedy, J. R.; Anderson, O. P.; Spertalian, K.; Dye, J. L. *Inorg. Chem.* **1987**, *26*, 724. (b) Swepston, P. N.; Ibers, J. A. *Acta Crystallogr.* **1985**, *C41*, 671. (c) Turowski, P. N.; Armstrong, W. H.; Roth, M. E.; Lippard, S. J. *J. Am. Chem. Soc.* **1990**, *112*, 681. (d) Gorun, S. M.; Lippard, S. J. *Recl. Trav. Chim., Pays-Bas* **1987**, *106*, 417.

Table 4. Product Distributions for the Oxidation of Alkanes and Phenol with *t*-BuOOH and H₂O₂, Catalyzed by Complexes **1** and **2**^a

entry	catal	oxidant	substrate	conversion of substrate (%)	product	yield ^c (%)	remark
1	1	<i>t</i> -BuOOH	cyclohexane	51.3	cyclohexanol	28.1	A/K ^d = 1.2
					cyclohexanone	23.2	KIE ^e = 1.8
2	2	<i>t</i> -BuOOH	cyclohexane	0	cyclohexanol	0	
					cyclohexanone	0	
3	1	30% H ₂ O ₂	cyclohexane	36.8	cyclohexanol	19.5	A/K = 1.1
					cyclohexanone	17.3	
4	2	30% H ₂ O ₂	cyclohexane	0	cyclohexanol	0	
					cyclohexanone	0	
5	1	30% H ₂ O ₂ + TBAB ^b	cyclohexane	47.6	cyclohexanol	25.4	A/K = 1.1
					cyclohexanone	22.2	
6	1	<i>t</i> -BuOOH	phenol	60.7	hydroquinone	59.8	
					quinone	0.9	
7	2	<i>t</i> -BuOOH	phenol	23.4	hydroquinone	23.4	
					quinone	0	
8	1	<i>t</i> -BuOOH	adamantane	50.7	1-adamantanol	47.6	3°/2° ^f = 15.4
					2-adamantanol	1.7	
					2-adamantanone	1.4	
9	1	<i>t</i> -BuOOH	<i>cis</i> -1,2-dimethyl-cyclohexane	38.8	<i>cis</i> -1,2-dimethyl-cyclohexanol isomers	20.2	<i>cis</i> / <i>trans</i> ^g = 1.1
					<i>trans</i> -1,2-dimethyl-cyclohexanol isomers	18.8	

^a Reactions were performed in acetonitrile solution under N₂ atmosphere. Reaction temperature: 35 °C. Reaction time: 2 h. *t*-BuOOH: *tert*-butylhydroperoxide. ^b TBAB: tetrabutylammonium bromide. ^c Yield based on the substrate. ^d A/K = cyclohexanol/cyclohexanone. ^e KIE = intermolecular kinetic isotope effect of cyclohexanol formation. ^f 3°/2° = (1-adamantanol)/(2-adamantanol + 2-adamantanone). ^g *cis*/*trans* = *cis*-1,2-dimethylcyclohexanol isomers/*trans*-1,2-dimethylcyclohexanol isomers = [(1*R*,2*R*)-1,2-dimethylcyclohexanol + (1*S*,2*S*)-dimethylcyclohexanol]/[(1*R*,2*S*)-1,2-dimethylcyclohexanol + (1*S*,2*R*)-dimethylcyclohexanol].

and *t*-BuOOH oxidant, where only the allylic product was observed.⁵⁰ The *cis/trans*-2-heptenes were converted to their corresponding epoxides in 72–76% yields with 93–97% retention of configuration (Table 5, entries 5 and 6). In the case of cumene, complex **1** gives only the 2-phenyl-2-propanol product. To the best of our knowledge, complex **1** is one of a few non-heme iron catalysts that are capable of catalyzing the oxidation of alkenes with epoxides as a main product.⁵¹ Complex **2** is not catalytic in the oxidation of all alkenes. Control experiments performed in the absence of catalyst **1** or in the presence of the ligand alone showed little or no oxidation. Autoxidation by Fe(NO₃)₃·9H₂O and FeCl₃·6H₂O was much slower and gave very low yields and selectivity. This indicates that the metal complex is required for the reactions to occur and is indeed acting as a catalyst.

Complex **1** efficiently catalyzes both the oxidation of cyclohexane and epoxidation of alkenes with *t*-BuOOH or H₂O₂ as the oxidant in good yields (36–85%) under mild conditions. Complex **2** has no catalytic activity toward the oxidation of cyclohexane and alkenes under the same conditions. The difference in catalytic activity between complexes **1** and **2** may be associated with the presence of the exchangeable ligands, methanol molecules and nitrate groups, in the diiron core of **1**. The methanol molecules trans to the bridged oxygen atom can be readily replaced by the oxidant or the substrate. This observation indicates that the presence of exchangeable ligands in non-heme iron catalysts provides the best catalytic activities, as reported in the literature.^{8b,11} The Cl⁻ in Fe–Cl bonds in **2** is not as labile,

which makes it a poor catalyst.^{11c} This is further supported by the efficient catalysis of the oxidation of phenol by both **1** and **2**. Apparently, phenol has strong coordinating ability and can replace Cl⁻ in complex **2**.⁵² A significant decrease was observed in the oxidation of cyclohexane by H₂O₂ compared to *t*-BuOOH, because complex **1** is less soluble in aqueous H₂O₂ than in the acetonitrile reaction mixture. This is underscored by the fact that the addition of the tetrabutylammonium bromide phase-transfer catalyst to the reaction mixture increases the oxidation.

It is worth pointing out that complex **1** slowly decomposes after 5 h and some precipitate was obtained in acetonitrile under reaction conditions. It is probable that the dinuclear oxo-bridged iron(III) core cleaved and two mononuclear iron species were formed during the reaction. This is further supported by the disappearance of the intense absorption band at ~542 nm after 5 h, which is assigned to ⁶A₁ → (⁴A₁, ⁴E) for a dinuclear μ -oxo-bridged motif (Figure 6). The characteristic absorption bands assigned to the π - π^* transition at 293 and 355 nm for the coordinated ligand are unchanged.

Mechanistic Probes of Alkane Oxidation. The alcohol/ketone (A/K) ratio is a simple test that probes the mechanism of alkane oxidation. Complex **1**'s A/K ratio is 1.2 with *t*-BuOOH and 1.1 with H₂O₂ (as shown in Table 4). Both values are close to 1, indicating that cyclohexane oxidation catalyzed by complex **1** involves either alkyl radicals with long lifetimes or [•]OH radicals.^{8b,53}

The intermolecular kinetic isotope effect (KIE) for the formation of cyclohexanol was determined in competition

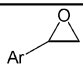
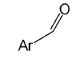
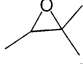
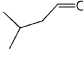
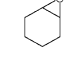
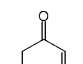
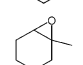
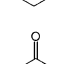
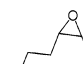
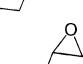


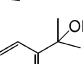
(50) Nam, W.; Ho, R.; Valentine, J. S. *J. Am. Chem. Soc.* **1991**, *113*, 7052.

(51) (a) White, M. C.; Doyle, A. G.; Jacobson, E. N. *J. Am. Chem. Soc.* **2001**, *123*, 7194. (b) Chen, K.; Costas, M.; Kim, J.; Tipton, A. K.; Que, L., Jr. *J. Am. Chem. Soc.* **2002**, *124*, 3026. (c) Guajardo, R. J.; Hudson, S. E.; Brown, J.; Mascharak, P. K. *J. Am. Chem. Soc.* **1993**, *115*, 7971.

(52) Gerloch, M.; McKenzie, E. D.; Towl, A. D. C. *J. Chem. Soc. A* **1969**, 2850.

(53) (a) Arends, I. W. C. E.; Ingold, K. U.; Wayner, D. D. M. *J. Am. Chem. Soc.* **1995**, *117*, 4710. (b) MacFaul, P. A.; Arends, I. W. C. E.; Ingold, K. U.; Wayner, D. D. M. *J. Chem. Soc., Perkin Trans. 2* **1997**, 135.

Table 5. Product Distributions for the Oxidations of Alkenes and Cumene with *t*-BuOOH, Catalyzed by Complex **1**^a

Entry	Substrate	Conversion of Substrate (%)	Product	Yield ^b %	Selectivity for Epoxide ^c	RC ^d
1	styrene	79.6		79.3	99.2%	
				0.3		
2	2-methyl-2-butene	84.5		83.9	98.6%	
				0.6		
3	cyclohexene	72.0		71.1	97.5%	
				0.9		
4	1-methylcyclohexene ^e	57.9		50.7	75.1%	
				7.2		
5	<i>cis</i> -2-heptene	81.2		76.9	96.7%	
				1.3		
6	<i>trans</i> -2-heptene	79.8		72.5	93.9%	
				2.3		
7	Cumene ^e	63.4		63.4		

^a Reactions were performed in acetonitrile solution under N₂ atmosphere. Reaction temperature: 35 °C. Reaction time: 3 h. ^b Yield based on the substrate. ^c Selectivity for epoxidation = epoxide product/(epoxide product + ketone or aldehyde product). ^d RC = 100(cis - trans)epoxide/(cis + trans)epoxide for epoxidation of *cis*-2-heptene or 100(trans - cis)epoxide/(cis + trans)epoxide for epoxidation of *trans*-2-heptene. ^e Reaction time: 2.5 h.

experiments between cyclohexane and [D₁₂]cyclohexane. A value of 1.8 (Table 4, entry 1) was obtained in acetonitrile, which is in the range of 1–2 for radical-type oxidations.⁵⁴

With adamantane as a substrate, a 3°/2° ratio of 15.4 (Table 4, entry 8) was observed. The selectivity for the oxidation at the tertiary position is higher than the average value of 2.7 found for Gif-type oxidations, about 2 for the oxidation of alkanes by •OH, and 9.5–10 for the oxidation with [Fe₂O(bpy)₄(H₂O)₂](ClO₄)₄/*t*-BuOOH.^{11b,55} It is in the range of 15–33 for oxidation with [Fe^{II}(TPA)(CH₃CN)₂]/H₂O₂^{9c,17a} and 11–48 for oxidation with PHIO catalyzed by P450 mimics.⁵⁶ These observations indicate that an oxidant

more selective than the hydroxyl radical is also involved in the oxidation.

The stereoselectivity of the alkane hydroxylation reaction was examined with *cis*-1,2-dimethylcyclohexane as a substrate, and the results are shown in Table 4 (entry 9). Both isomeric *cis*-1,2-dimethylcyclohexanol and *trans*-(1*R*,2*S* or 1*S*,2*R*)-1,2-dimethylcyclohexanol were formed with a *cis*/*trans* ratio of 1.1, which is in the range of 1.1–1.3 found for a catalytic autoxidation reaction.⁵⁷ This indicates the formation of alkyl radicals with a lifetime sufficient to allow epimerization at the radical site.

The data imply that alkyl radicals are involved in the oxidation of the alkanes studied here, although it does not exclude the possibility that a metal-based oxidant is also

(54) Kehenkim, A. M.; Shilov, A. E. *New J. Chem.* **1989**, *13*, 659.

(55) Ménage, S.; Vincent, J.-M.; Lambeaux, C.; Fontecave, M. *J. Mol. Catal., A* **1996**, *113*, 61.

(56) Groves, J. T.; Nemo, T. E. *J. Am. Chem. Soc.* **1983**, *105*, 6243.

(57) Miyjima, S.; Simamura, O. *Bull. Chem. Soc. Jpn.* **1975**, *48*, 526.

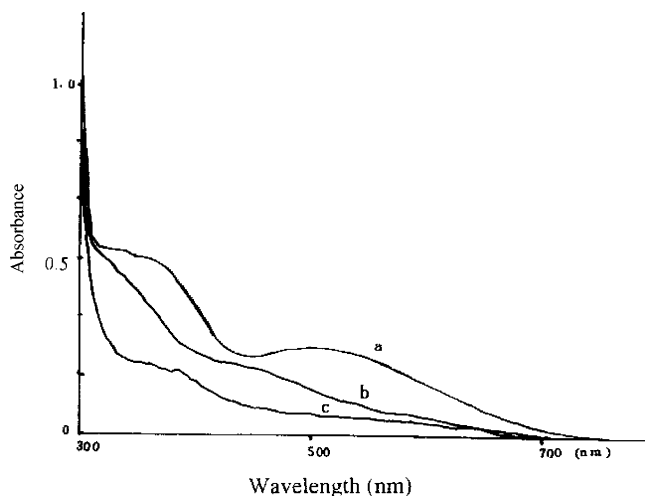


Figure 6. UV/vis spectra of catalyst **1** at various reaction times: (a) at time zero; (b) after 1 h; (c) after 5 h.

involved in the oxidation because of a higher $3^\circ/2^\circ$ ratio of 15.4 for the oxidation of adamantane.

As far as the oxidation of alkenes is concerned, complex **1** exhibits highly stereoselective epoxidation of the alkenes studied, indicating a type of two-electron oxidation process^{51b} and involvement of a metal-based oxidant.⁵⁸ With styrene as a substrate, complex **1** afforded almost all epoxide product with very little benzaldehyde, which is derived from the O₂ trapping of a radical cation species,⁵⁹ and points to the involvement of a nonradical oxidant. The oxidation of 1-methylcyclohexene with *t*-BuOOH gave 75% epoxide product and 25% ketone product. With cyclohexene, which is susceptible to allylic oxidation, 99% epoxide product was found and little ketone product was observed. These results indicate that a nonradical oxidant is involved in the oxidations. In the oxidations of *cis/trans*-2-heptenes both compounds were converted into their corresponding *cis/trans*-epoxides with 93–98% retention of configuration. This high degree of retention of configuration is consistent with a nonradical mechanism^{51b} or, less likely, with a radical mechanism having very short-lived radical intermediates. Complex **1** also gave only 2-phenyl-2-propanol product in the oxidation of cumene under our standard reaction conditions, indicating involvement of a metal-based oxidant intermediate in the oxidation.⁶⁰ These results indicate that nonradical species, probably metal-based intermediate oxidants, are involved in the oxidations of the alkenes studied and cumene.

On the basis of the data above, we suggest that two different oxidants (RO[•] and iron–oxo) might be involved

in the oxidations^{55,61} and we propose the following possible mechanism. In the first step of the reaction, the binding of the oxidant to the dinuclear complex results in the cleavage of the dinuclear unit into monomers, forming an LFe^{III}–OOR intermediate. This unstable peroxy complex would either generate an Fe^{IV}=O and the highly reactive RO[•] by O–O bond homolysis or generate a hypervalent oxo–iron intermediate Fe^V=O by bond O–O heterolysis, or it could simultaneously generate all reactive species both by O–O bond homolysis and heterolysis. A transient species Fe^V=O with a non-heme macrocyclic ligand was recently isolated and fully characterized by X-ray diffraction,⁶² showing that non-heme ligands can stabilize the Fe^V=O transient species. In the case of the oxidation of alkenes, the O–O bond heterolysis predominates, which results in Fe^V=O active oxidizing intermediates. This is followed by the intermediate Fe^V=O transfer of oxygen atoms to alkenes, giving epoxides as major products. It is possible that the nucleophilic nature of the C=C bonds in alkenes favors the formation of Fe^V=O transient species, resulting in the Fe^V=O intermediates domination of the oxidations of alkenes. With the oxidations of alkanes, O–O bond homolysis dominates and generates reactive alkoxy radicals RO[•] that are involved in the oxidation of alkanes. This is in good agreement with the 1:1 ratio of cyclohexanol/cyclohexanone during the oxidation of cyclohexane. However, more experiments are needed to confirm the validity of this proposed mechanism.

Conclusions

To prepare functional models that can mimic the alkane functionalization chemistry of methane monooxygenase, the dinuclear oxo-bridged complex **1** was synthesized with the planar tridentate 2,6-bis(*N*-methylbenzimidazol-2-yl)pyridine, L, and Fe(NO₃)₃·9H₂O or [Fe₃O(OAc)₆(H₂O)₃]NO₃ in methanol solution. Mononuclear complex **2** was also obtained by reaction of L with (NEt₄)₂(Fe₂OCl₆). Crystallographic studies revealed that each Fe(III) in [Fe₂OL₂(MeOH)₂(NO₃)₂](NO₃)₂ (**1**) has a distorted octahedral geometry containing a N₃O₃ donor set with three N atoms from L and three O atoms from nitrate, methanol, and a bridged oxo unit. In FeLCl₃, **2**, Fe(III) is coordinated to three N atoms from L and three Cl[−] anions. Complex **1** is the first example of a structurally characterized linear, dinuclear, oxo-bridged complex with a planar tridentate ligand containing a methanol coordinated trans to the μ -oxo bridge. In catalytic studies, complex **1** displays high catalytic activity in the oxidation of alkanes and is an excellent catalyst for stereoeoxidation of the alkenes studied, while complex **2** is inactive. The difference in catalytic activity between complexes **1** and **2** shows that the presence of a labile coordinated group is essential to

(58) (a) Arasasingham, R. D.; He, G.-X.; Bruce, T. C. *J. Am. Chem. Soc.* **1993**, *115*, 7985. (b) Wessel, J.; Crabtree, R. H. *J. Mol. Catal.*, A **1996**, *113*, 13.
(59) (a) Heimbrook, D. C.; Carr, S. A.; Mentzer, M. A.; Long, E. C.; Hecht, S. M. *Inorg. Chem.* **1987**, *26*, 3835. (b) Groves, J. T.; Gross, Z.; Stern, M. K. *Inorg. Chem.* **1994**, *33*, 5065.
(60) Minisci, F.; Fontana, F.; Araneo, S.; Recupero, F.; Banfi, S.; Quici, S. *J. Am. Chem. Soc.* **1995**, *117*, 226.

(61) (a) Nishida, Y.; Okuno, T.; Ito, S.; Harada, A.; Ohba, S.; Matsushima, H.; Tokii, T. *Chem. Lett.* **1995**, 886. (b) Sheu, C.; Sawyer, D. T. *J. Am. Chem. Soc.* **1990**, *112*, 8212. (c) Kulkova, V. S.; Gritsenko, O. N.; Shiteinman, A. A. *Russ. Chem. Bull.* **1995**, *44*, 2415. (d) Ménage, S.; Vincent, J.-M.; Lambeaux, C.; Fontecave, M. *J. Chem. Soc., Dalton Trans.* **1994**, 2081. (e) Shilov, A. E.; Shiteinman, A. A. *Acc. Chem. Res.* **1999**, *32*, 763.
(62) Rohde, J.-U.; In, J.-H.; Lim, M. H.; Brennessel, W. W.; Bukowski, M. R.; Stubna, A.; Münck, E.; Nam, W.; Que, L., Jr. *Science* **2003**, *299*, 1037.

permit the oxidant or substrate to bind to the Fe for an efficient catalyst. Mechanistic studies show that the mechanism of catalytic oxidation by complex **1** depends on the substrates used: a A/K ratio (close to 1) and a low KIE value (1.8) for cyclohexanol formation as well as the lack of stereoselectivity in the oxidation of *cis*-dimethylcyclohexane suggest that alkyl radicals are involved in the oxidation. Stereospecific epoxidation of the alkenes studied, stereoselectivity of the oxidation of cumene, and the high degree of retention of configuration in the oxidation of *cis/trans*-2-heptenes indicate that nonradical species, probably metal-based intermediate oxidants, are involved in the oxidations of the alkenes and cumene.

Acknowledgment. We wish to thank the National Institutes of Health (NIH) MBRS SCORE Program (Grant

No. 1 S06 GM 63119-01) for financial support. Partial support from the Research Corp. (Grant No. CC5392) and the Petroleum Research Fund administered by the American Chemical Society (Grant No. 37034-GB3) are also acknowledged. E.B.S. wishes to thank the Arnold and Mabel Beckman Foundation for a Beckman Scholar's Award and the Howard Hughes Medical Institute (Grant No. 52002663). We thank Professor Henry Po (CSULB), Professor A. Guy Orpen (Bristol) and the reviewers for their comments.

Supporting Information Available: Tables of crystal data and structure solution, refinement details, atomic coordinates, bond lengths and angles, and anisotropic thermal parameters for compounds **1** and **2**. This material is available free of charge via the Internet at <http://pubs.acs.org>.

IC0259437